

## GROUND-BASED RADAR INTERFEROMETRY FOR MONITORING UNSTABLE SLOPES

*Massimiliano Pieraccini, Guido Luzi, Daniele Mecatti, Linhsia Noferini, Giovanni Macaluso,  
and Carlo Atzeni*

*University of Florence*

*Department of Electronics and Telecommunications*

*via Santa Marta 3 50139 Firenze, Italy*

*e-mail: [massimiliano.pieraccini@unifi.it](mailto:massimiliano.pieraccini@unifi.it)*

**Abstract:** A ground-based coherent radar instrumentation acquires a time series of radar images. The complex product, pixel by pixel, of a pair of holographic radar images, taken at different moments, gives an interferogram whose phase is related to pixel distance from the sensor. When terrain displacements occur in the time elapsed between two image acquisitions, the phase of the corresponding pixel will vary accordingly. Ground-based radar interferometry is a powerful technique for monitoring terrain deformation on unstable slopes. In this paper the technique is briefly described with reference to some recent experimental cases, reviewing in its potentials and limits. In spite of its indubitable advantages, a number of potential error sources have been recognized: instrumentation instability, repeatability of the measurements after removal and further reinstallation of the instrumentation, atmospheric path delay changes, temporal decorrelation of the scenario, and phase wrapping. All these limits can be overcome by suitable solutions (atmospheric corrections, coherent points analysis, phase unwrapping techniques) that will be discussed in this paper.

### 1. Introduction

The history of Ground Based SAR Interferometry, a spin-off from the differential microwave interferometry from space (DInSAR) can be considered originated in 1998 [1] and during the subsequent years, several experimental campaigns were carried out, mainly devoted to monitor landslides and instable slopes [2] [3] [4]. The success of this application rapidly increased up to now, including its application for volcanoes [5] and snow cover [6] monitoring. At the moment the technique, when images are collected continuously, can be considered so consolidated that the characteristics of the motion of the observed scenario can be evaluated. When measurements are separated by long time lapse, the technique can suffer from temporal discontinuity and specific processing techniques must be applied to obtain reliable data [7]. In this paper examples of results obtained in these different situations are presented.

## 2. Principle of Differential SAR Interferometry

Conventional pulse radar resolves targets in the range direction by measuring the time it takes a pulse to propagate to the target and return to the radar, after the backscattering process has taken place. Targets that differ from each other in their azimuth/cross-range coordinates only, generate overlapping radar echoes and thus they cannot be distinguished. Azimuth location can be achieved by changing the viewing angle of a directive antenna and processing the range information relative to each angle separately. To accomplish Synthetic Aperture, complex radar data, amplitude and phase, provided by an antenna that moves across a defined series of positions can be processed, and the region of interest is observed from a sequence of spatial sampling positions. The received signals are combined using focusing algorithms, aimed at obtaining high resolution along the antenna track direction. The generated images reproduce the location and the reflectivity of a surface in a two-dimensional coordinate system, with one axis along the antenna track direction (“azimuth” or “cross range” direction) and the other orthogonal to the first axis and pointing toward the radar line of sight direction (“cross-track” or “range” direction).

The third dimension is not available and the effect on SAR images depends on the relative geometry of the SAR aperture and the illuminated surface. Target locations can be distorted relative to a plan metric view and their identifications could be very difficult. The radar image can then be projected on the Digital Elevation Model of the observed scenario, obtaining a 3D view of the scene. An example of a 3D SAR power image compared with the corresponding photo is shown in fig. 1.

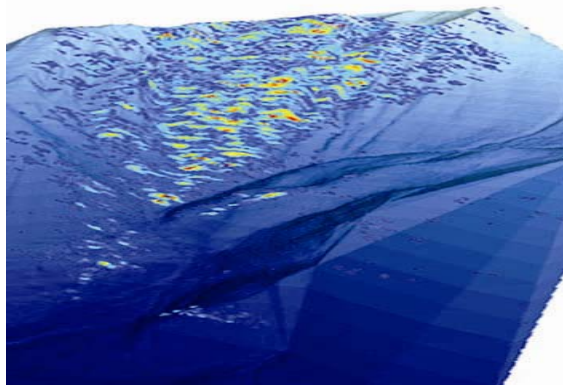


Figure 1a: an example of a SAR image projected on the DEM. After[10].



Figure 1b: photo roughly correspondent to the scene of fig. 1a.

The phase of the conjugate product between two complex radar images of the same surface area, acquired at different times, builds up a radar interferogram which can be used in SAR interferometry to determine the occurred range variations. This is usually implemented by multiplying the complex reflectivity at each point of one image by its corresponding conjugate value in the second image, so that the interferogram also preserves useful information about the signal amplitudes. The complex product effectively cancels out the common backscattering phase in each resolution element leaving the phase term proportional to the difference between the path delays.

When the positions of the elemental scatterers within resolution element change it can yield a global delay appreciable as a change of  $r$  but leaving nearly unchanged the coherent backscattering coefficient. In this case the retrieved range variation is the projection along the range direction of the net cell displacement and is the matter of terrain displacement mapping.

If significant variations of the scatterers position, dielectric phase response or other effects due to propagation occur, the global change of the phase of the pixel, can not be longer simply associated to a range modification. The application of interferometry is strongly related to the evaluation of a parameter, the correlation coefficient, defined by the following expression.

$$\gamma = \frac{\langle I_1 \cdot I_2^* \rangle}{\sqrt{\langle I_1 \cdot I_1 \rangle \langle I_2 \cdot I_2 \rangle}} = G e^{j\theta} \quad (1)$$

$I_1$  and  $I_2$  represent the two SAR images, the brackets  $\langle \cdot \rangle$  mean the average value of the argument and  $\theta$  is the corresponding interferometric phase. The interferometric coherence is the amplitude  $G$  of the correlation coefficient  $\gamma$  between the two complex SAR images forming the interferogram. The variance of the measured phase is related to the amplitude of  $\gamma$ , coherence, equivalent to fringes visibility usually considered in optical interferometry. When phase variation due to dielectric behaviour of the media is negligible, considering single pixels which contains many scatterers, coherence estimates how in the occurred variation within the pixel, the mutual position of the scatterers has maintained. If the displacements between two images randomize the positions of each scatterer with respect to others, the pair of echoes will be less well related and the coherence of the interferogram will decrease resulting in a noise that may mask the underlying phase signature.

When the two images from which the differential phase is retrieved are separated by a long time interval, the loss of coherence can reduce the reliability of the results; several papers deal with this topic in the field of microwave interferometry from space [8] and more recently from ground-based radar observations [9] [10]. So radar images acquired at different dates can be fruitful for differential interferometry only if the temporal coherence among different images does not decrease much below the unity value.

To evaluate the echo decorrelation we can consider the simple scheme proposed in [11] and analyse it for ground based approach. Considering the effect of dielectric variations of the observed media affecting the differential phase of the backscattered echoes negligible, the measured differential phase,  $\varphi_{\text{Measured}}$  can be considered as the summation of four terms:

$$\varphi_{\text{Measured}} = \varphi_{\text{Instr}} + \varphi_{\text{Atm}} + \varphi_{\text{Geom}} + \varphi_{\text{Disp}} \quad (2)$$

Here  $\varphi_{\text{Instr}}$  resumes the instrumental noise,  $\varphi_{\text{Atm}}$  comes from atmospheric effects;  $\varphi_{\text{Geom}}$  is the contribution of geometric decorrelation which in ground based case concerns only the mechanical stability of the system (zero baseline condition), and finally  $\varphi_{\text{Disp}}$  is the term due to the actual displacement. We briefly give a summary of some observations useful for the specific case of GB SAR Interferometry.

The term,  $\varphi_{\text{Instr}}$ , comes from instrumental decorrelation: the phase measured by the transceiver can be affected by errors due to the temporal instability of the frequency of the transmitter and the thermal and mechanical stress on the Radio Frequency cables and components. A critical point is the stability of phase over long time interval from several weeks or months,

i.e. for different campaigns. In order to overcome the shortcomings due to temporal and geometrical decorrelation in a long term, not continuous campaign, sophisticated processing techniques as the Permanent Scatterers PS<sup>TM</sup>, introduced in [7] for space DInSAR, allowed to overcome this drawback, by using sparsely distributed but phase stable point targets, called “persistent scatterers”.

Satellite data at C band demonstrated phase retrieval can be strongly affected by atmospheric state too. The cause of this additional delay,  $\varphi_{\text{atm}}$ , is the deviation of the speed of the radar wave from the constant value in vacuum,  $c$ , to  $c/n$  where  $n$  is atmosphere refractive index, which depends on air humidity,  $U$ , temperature,  $T$ , and pressure,  $p$ , in order of importance. Other effects as ionospheric disturbances are absent in ground based measurements. At lower frequencies the delay induced by atmosphere corresponds to a smaller phase term but variation of interferometric phase due to atmospheric fluctuations can be compared with the other decorrelation sources. The uncertainty introduced can be comparable to the required accuracy on displacement measurement.

The third term to be considered in eq. 2 comes from geometric decorrelation. In GB SAR the radar system remains in the same spatial position, maintaining the same geometrical path. Sometimes, when time between to subsequent campaigns is long and at the end of each campaign the radar system, including the mechanical frame, is dismantled, the subsequent repositioning can be subject to error due to mechanical tolerance and to introduce a geometric decorrelation; a careful check of the repositioning, carried out for example through single accurate optical measurements, is usually adequate to assure a millimetre accuracy.

When the SAR images used for interferometric mapping are acquired with temporal separation of months, the influence of this phase disturbance on GB-SAR interferometric measurements must be properly investigated [12]: a possible solution for ground based long term decorrelation is derived from the application of the Permanent Scatterers technique in a specific development for ground based case [10].

The interferometric phase signatures vary relatively smoothly from point to point in the interferogram and may be inverted to recover displacement along the line of sight (LOS). However, the phase observables are measured modulo  $2\pi$ ; that is, the integral number of phase cycles on each measurement is lost. It is said that the phase values, which varies linearly with range, are wrapped in the interval  $[-\pi, \pi)$  by the measurement process. Consequently, if the surface displacement in a scene determines a phase excursion greater than one cycle, the interferogram cannot be uniquely inverted without a procedure to recover the missing cycles. Such procedures are referred as phase unwrapping [13].

When decorrelation effects are negligible, the phase  $\varphi$  of each image pixel contains information about pixel distance from the sensor and if a terrain displacement occur in the time elapsed between two SAR acquisitions, the phase will vary accordingly. The displacement map is obtained taking the phase of the corresponding interferogram. For our purpose it results advantageous to calculate the cumulative interferogram instead of the standard interferogram. Let  $I_1, I_2, I_3, \dots, I_N$  be a set of radar images acquired at  $t_1 < t_2 < t_3, \dots < t_N$  times respectively. The cumulative interferogram of this set is defined as:

$$\varphi_{1,N} = \sum_{i=1}^{N-1} \angle(I_{i+1}(\cdot)I_i^*(\cdot)) = \sum_{i=1}^{N-1} \angle(e^{j(\varphi_{i+1}(\cdot) - \varphi_i(\cdot))}) \quad (3)$$

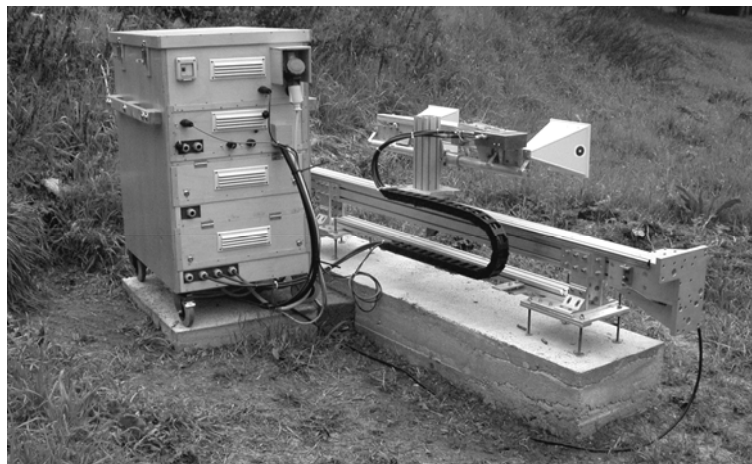


Figure 2: the radar system.

where ‘ $*$ ’ is the complex operator and  $\angle(I_k) = \varphi_k$ .

This approach offers two advantages: first, always considering phase changes between two consecutive SAR images, phase wrapping is most unlikely; then by summing all the partial contributions, possible white noise is reduced.

By assuming dielectric characteristics of the pixel point  $n$  are the same for each observation time, supposing the atmospheric contribution is removed, the displacement  $\Delta r_n$  of the point  $n$  is recovered from the cumulative interferogram by the following equation:

$$\Delta r_n = \frac{\varphi_{1,N}}{4\pi} \lambda \quad (4)$$

where  $\lambda$  is the central wavelength.

The expected order of magnitude of displacement and the velocity of the landslide ask for the optimal choice of the operating frequency. When the echo propagates from the radar to the target and back in a perfect dielectric, the phase of its electromagnetic wave varies proportionally to the displacement. An optimal choice of the wavelength results from a trade-off between the shortest value able to assure the required displacement precision and the largest one avoiding phase wrapping due to fast movements, i.e. displacements which in the time occurred between two image acquisition exceed the length of one wavelength.

In this paper data obtained by using a centimetre wavelength, which corresponds to a frequency belonging to C band, are discussed.

### 3. The measuring system

The employed ground based radar instrumentation mainly consists of a continuous-wave step-frequency (CW-SF) transceiver working at C band, a linear horizontal rail where the antennas move for scanning the synthetic aperture, and a PC controlling the transceiver, the antenna motion and data recording. Fig. 2 shows a photo of the instrumentation. In order to compensate for the phase shifts produced by mechanical and thermal deformations of the cables, a auto-calibration procedure, was designed. For each rail position, two measurements are carried out in sequence: first the signal backscattered by the illuminated scene is acquired through the microwave path from the receiving antenna, later the signal from the receiver unit is acquired through the internal path: in this way normalized data, which are not affected by thermal and mechanical cable deformations are obtained. For the measurement campaigns

usually the radar system is located on a suitably built platform, ensuring a good visibility of the main flows of the landslide within a maximum distance of 2 Km. Measurement configuration influences on spatial resolution of the retrieved images: in table 1 the main parameters used during Citrin campaign (cfg. Fig.1 ), discussed in the following paragraph, are resumed.

Measurement parameters	
Target distance m	1000-2000m
Transmitted Power	20 dBm
Band	30 MHz
Central frequency	5.85 GHz
Polarisation VV	VV
Antenna gain	15 dB
Frequency number	801
Linear scansion length	1.8 m
Linear scansion point number	161

Table 1: Measurement parameters used during Citrin Campaign [10].

#### 4. Examples of data collection

In the last years the radar apparatus available at the Department of Electronic and Telecommunications of the University of Florence, was used in several campaigns to monitor different situations. Hereafter three examples of the application of the technique, are shown; two were obtained with continuous measurements (Tessina landslide and Belvedere Glacier), leaving the radar system fixed for one/two weeks. A further example is shown where a long time interval, several months, separates the different acquisitions (Citrin valley).

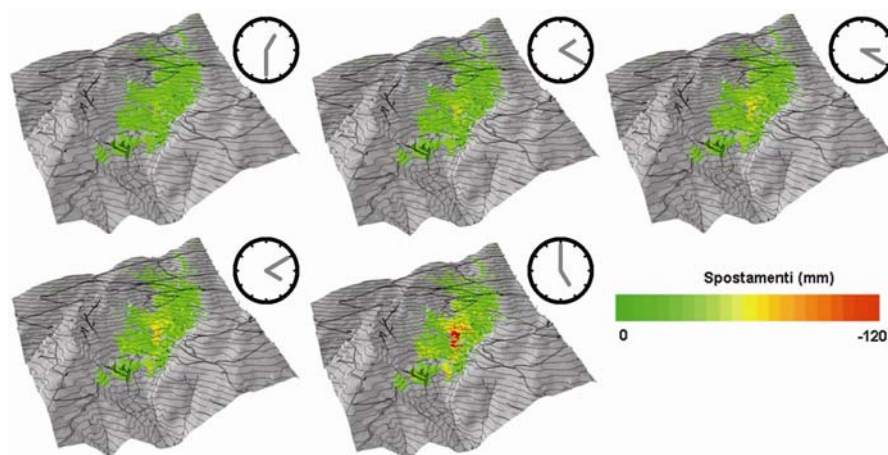


Figure 3: temporal behaviour of the displacement maps in mm, obtained on Tessina landslide. Negative values refer to motion towards the radar position. Clock ikons represent the running time, lasting overall 3 hour and half.

##### 4.1. Tessina landslide

The Tessina landslide, is located on the southern slopes of Mount Teverone, in the Alpage valley in north-east Italy. This landslide was previously monitored by means of a ground-based DInSAR system in 2000: for the description of the performed activities see [4]. A more recent experimental campaign, was carried out in June 2004 with an apparatus working at a different frequency (C band) [14]. The monitored area consists of a large, highly active, complex gravitational. The landslide, which first became active in 1960, now threatens two

villages, and is hence subject to careful monitoring by collecting a large mass of movement data. The landslide extends from an elevation of 1200 m a.s.l at the crown down to 610 m a.s.l. at the toe of the mudflow. The values retrieved from radar data were validate through standard instrumentation (theodolite). Typical displacements maps, projected on the DEM, are shown in fig.3 .

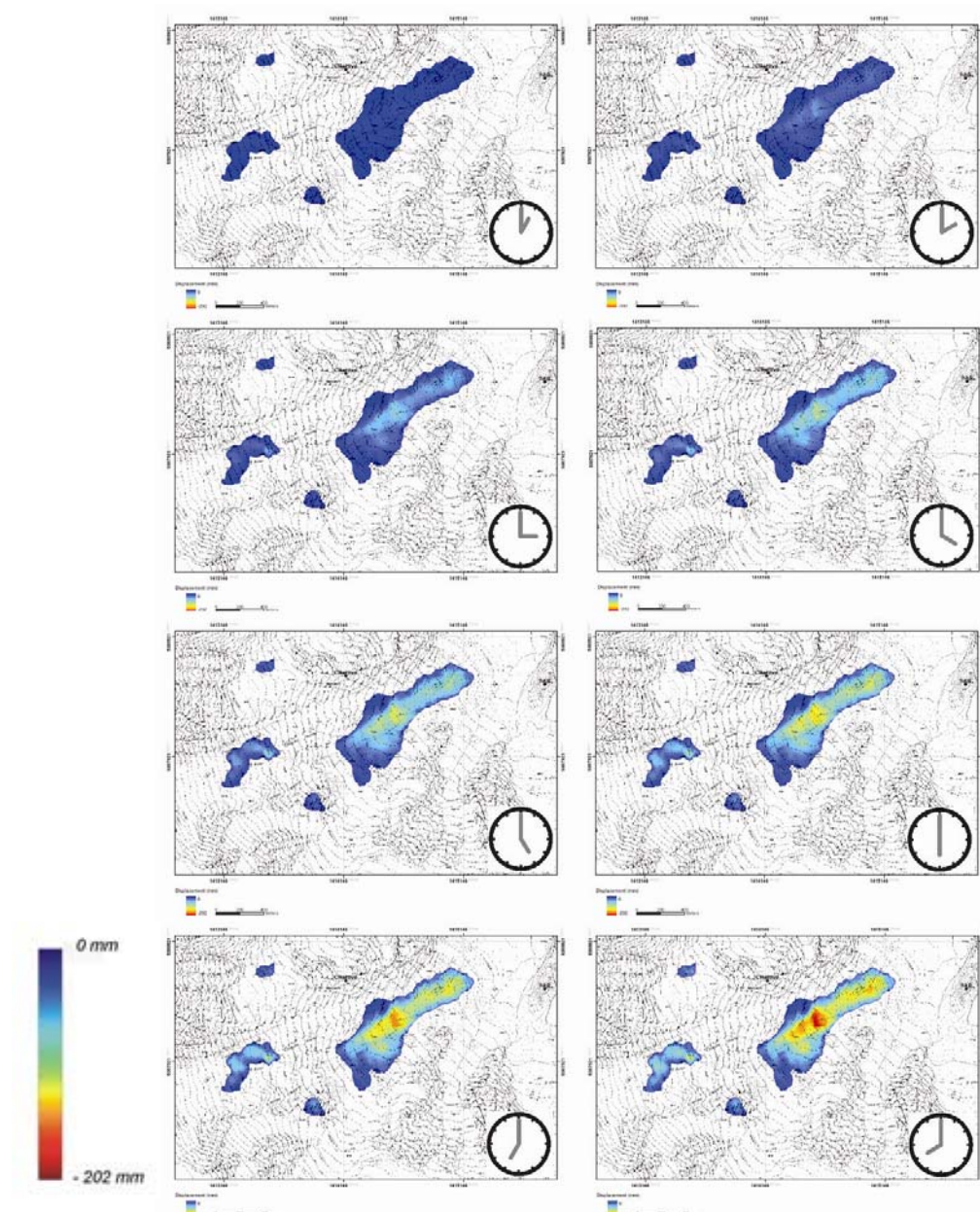


Figure 4: temporal behaviour of the displacement maps in mm, obtained on Belvedere glacier. Negative values refer to motion towards the radar position. Clock ikons represent the running time, lasting 8 hours.

## 4.2. Belvedere glacier

More recently an experiment was carried out to monitor a glacier: the lobe of the glacier Belvedere, one of the largest glaciers of the Alp mountains, just close to the town of Macugnaga. In the last years all the around area has suffered from geological instabilities generating a continuous and anomalous amount of debris mixed with ice that greatly feeds the lobe down to the plain. Now attention is turned to some landslides from the middle of the oriental slope of Monte Rosa that increased the silt on the large glacier at the basis of the mountain slope.

The measurement campaign, started on 26 of August 2004 and lasted about a week. The antenna viewing angle is  $25^\circ$  to the horizontal plane and allowed to illuminate the middle of the mountain slope.

The instrumentation was used with the measurement parameters similar to those used for Tessina summarized in table 1. The monitored area is an heterogeneous surface affected by debris flow, ice falls and small avalanches. The first outcome from the measured data is that the glacier moves so fast that phase wrapping occurs when two subsequent images are compared, even if only 36 minutes elapsed.

Fig. 4 shows a result of the monitoring of the glacier, consisting of a set of displacement maps acquired at different times (total 8 hours) after the wrapping removal was applied. The detected motion reveal a high velocity but comparable with the values expected for this kind of glaciers during the ablation season. Apart from the occurrence of phase wrapping, the coherence maintained high for the entire duration of the experiment(8 days).

## 4.3. Citrin valley

Citrin valley is located in the Gran San Bernardo mountains in the Alps of Valle d'Aosta, Italy. In recent years, the southern part of this valley has suffered from the effects of landslides. In particular, as a consequence of some heavy precipitation events in October 2000, new large landslides occurred. GB-SAR observations were carried out with the collaboration of Cesi spa (former ENEL.HYDRO company) and the Valle d'Aosta authority, at the end of September 2003 and then repeated on July 2004.

In this case due to the long time elapsed between different collected images, a method to recover coherence as far as a finite number of points was applied. The method used to identify possible PS points is based on the analysis of the time series of their amplitude values. This approach is due to the fact that an exact evaluation of the phase stability is possible only after estimation and removal of the atmospheric contribution, while amplitude values are almost insensitive to the atmospheric phenomena. A simple relationship was inferred between atmospheric effect and interferometric phases that can be used generally to describe the observed interferometric phase variations [10]. The result retrieved from the data of the two campaigns, separated by a temporal baseline of ten months, are shown in Fig.5 where the displacements measured on the PSs pixels are reported. The enumerated points on the figure are points also monitored by a GPS network installed by Cesi spa (former ENEL.HYDRO company). The agreement between displacements retrieved from interferometric data and GPS estimation is fine even if the test was limited to a few GPS measurements.



## 5. Conclusions

GB SAR Interferometry, thanks to its short measurement time is able to provide not only displacement but also velocity field estimation with great aid for the assessment of the risk of the monitored areas. The retrieval of motion characteristics of a monitored slope is consolidated when instrumentation is used in continuous way. In the other case, when the temporal interval is so long to reduce the coherence between the considered images, by means of a PS analysis, we can identify an ensemble of coherent points on the scene, then study these points with the aim of investigating, and possibly removing, the atmospheric influences on their interferometric phases. With this method inferred from space application, the potential of this technique is huge: unstable slopes can be remotely monitored without installation of sensors directly on the slope providing a unique effective alternative solution to satellite survey.

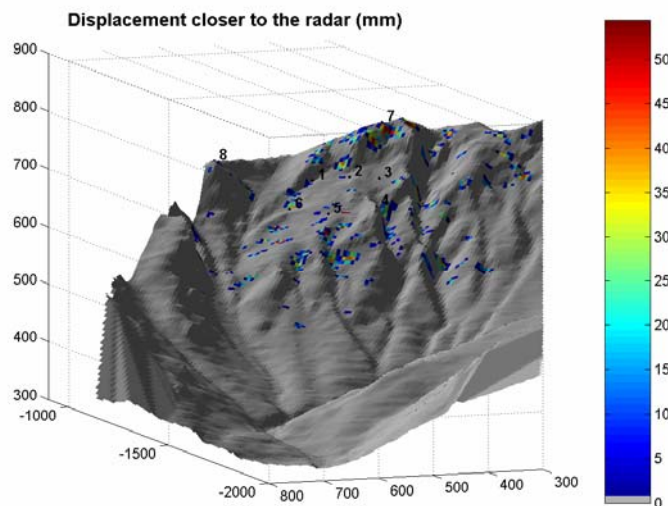


Figure 5: Citrin, comparison between the two campaigns: Measured displacement closer to the radar relative to the PSs pixels. The points labelled by 1,...,8 are points monitored by the GPS network

## References:

- [1] D. Tarchi, H. Rudolf, G. Luzi, L. Chiarantini, P. Coppo, and A. J. Sieber, "SAR interferometry for structural changes detection: A demonstration test on a dam", in Proc. IGARSS, 1999, pp. 1522–1524.
- [2] D. Leva, G. Nico, D. Tarchi, J. Fortuny, and A. J. Sieber, "Temporal Analysis of a Landslide by Means of a Ground-Based SAR Interferometer", IEEE Trans. Geosci. Remote Sensing, vol. 41, no. 4, pp 745-752, April 2003.
- [3] Pieraccini, M., Casagli, N., Luzi G., Tarchi, D., Mecatti, D., Noferini, L., And C. Atzeni, 2002, Landslide monitoring by ground-based radar interferometry: a field test in Valdarno (Italy). International Journal of Remote Sensing, 24 6, pp. 1385-1391.
- [4] Tarchi, D., Casagli, N., Fanti, R., Leva, D., Luzi, G. Pasuto, A., Pieraccini, M., Silvano, S., 2003, Landside Monitoring by Using Ground-Based SAR Interferometry: an example of application to the Tessina landslide in Italy, 1. Engineering Geology 68, pp.15-30

- [5] D. Leva, "Landslides and Volcanoes monitoring by LiSA", 2004, Proceedings of the URSI Comm. F Workshop., Symposium on Microwave Remote Sensing of the Earth, Ocean, Ice and Atmosphere, 20-21 April, Ispra – Italy.
- [6] Vazquez M., Fortuny J.G., 2004, Monitoring structural changes and Stability of the snow cover with a Ground-based Synthetic Aperture Radar, Proceedings of the URSI Comm. F Workshop., Symposium on Microwave Remote Sensing of the Earth, Ocean, Ice and Atmosphere, 20-21 April, Ispra – Italy.
- [7] Ferretti, A., Prati, C., Rocca, F. 2001, Permanent Scatterers in SAR Interferometry. IEEE Trans. on Geosci. and Remote Sensing, 39 1, pp. 1685-1701.
- [8] Zebker, H. A. And J.Villasenor, 1992, Decorrelation in Interferometric Radar Echoes. IEEE Trans. on Geosci. and Remote Sensing, 30, pp. 950-959 .
- [9] Luzi, G., Pieraccini, M., Mecatti, D., Noferini, L., Guidi, G., Moia, F. And C. Atzeni, 2004, Ground-based radar interferometry for landslides monitoring: atmospheric and instrumental decorrelation sources on experimental data. IEEE Trans. on Geosci. and Remote Sensing, 42 11, pp. 2454- 2466.
- [10] Noferini L., Pieraccini M., Mecatti D., Luzi G, Tamburini A. And Carlo Atzeni, 2005, Permanent scatterers analysis for atmospheric correction in Ground Based SAR Interferometry , IEEE Trans. on Geosci. and Remote Sensing. IEEE Trans. on Geosci. and Remote Sensing, Vol. 43 Issue: 7, July.2005 Pages: 152-157.
- [11] Kenyi, L.W. And Kaufmann, V., 2003, Estimation of Rock Glacier Surface Deformation Using SAR Interferometry Data. IEEE Trans. on Geosci. and Remote Sensing, 41 6, pp. 1512-1515.
- [12] Bamler, R. And Just, D., 1993, Phase statistics and decorrelation in SAR interferograms. In Proc. of the Geoscience and Remote Sensing Symposium IGARSS '93, ' Better Understanding of Earth Environment', Tokio, Japan , vol. 3 pp. 980 - 984.
- [13] R. M. Goldstein, H. A. Zebker, and C. L. Werner, 1988, "Satellite Radar Interferometry: Two-dimensional Phase Unwrapping", Radio Scienc, vol. 23, no. 4, pp. 713-720, July.
- [14] Luzi G. , M. Pieraccini , D. Mecatti, L. Noferini, G. Macaluso, A. Galgaro C. Atzeni Advances in ground-based microwave interferometry for landslide survey: a case study, accepted for publication in International Journal of Remote Sensing.